PROCEEDINGS OF SPIE

SPIEDigitalLibrary.org/conference-proceedings-of-spie

Effects of iron-oxide nanoparticles on compound biofilms of streptococcus gordonii and fusobacterium nucleatum

Jane Nguyen, Nathan Withers, Gema Alas, Arjun Senthil, Christina Minetos, et al.

Jane Q. Nguyen, Nathan J. Withers, Gema Alas, Arjun Senthil, Christina Minetos, Nikita Jaiswal, Sergei A. Ivanov, Dale L. Huber, Gennady A. Smolyakov, Marek Osiński, "Effects of iron-oxide nanoparticles on compound biofilms of streptococcus gordonii and fusobacterium nucleatum," Proc. SPIE 10507, Colloidal Nanoparticles for Biomedical Applications XIII, 105070J (23 February 2018); doi: 10.1117/12.2299280

SPIE.

Event: SPIE BiOS, 2018, San Francisco, California, United States

Effects of iron-oxide nanoparticles on compound biofilms of *Streptococcus gordonii* and *Fusobacterium nucleatum*

Jane Q. Nguyen[1], Nathan J. Withers[1], Gema Alas[1], Arjun Senthil[1], Christina Minetos[1], Nikita Jaiswal[1], Sergei A. Ivanov[2], Dale L. Huber[3], Gennady A. Smolyakov[1], and Marek Osiński[1]

[1]Center for High Technology Materials, University of New Mexico, 1313 Goddard St. SE, Albuquerque, NM 87106-4343, USA
[2]Center for Integrated Nanotechnologies, Los Alamos National Laboratory, 1000 Eubank SE, Albuquerque, New Mexico 87123, USA
[3]Center for Integrated Nanotechnologies, Sandia National Laboratories, 1000 Eubank SE, Albuquerque, New Mexico 87123, USA

ABSTRACT

The human mouth is a host of a large gamut of bacteria species, with over 700 of different bacteria strains identified. Most of these bacterial species are harmless, some are beneficial (such as probiotics assisting in food digestion), but some are responsible for various diseases, primarily tooth decay and gum diseases found in gingivitis and periodontitis. Dental plaque comprises a complicated biofilm structure that varies from patient to patient, but a common factor in most cases is the single species of bacterium acting as a secondary colonizer, namely *Fusobacterium nucleatum*, while the actual disease is caused by a variety of tertiary colonizers. We hypothesize that the destruction of a compound biofilm containing *F. nucleatum* will prevent tertiary colonizers from establishing a harmful biofilm, and thus will protect the patient from developing gingivitis and, consequently, periodontitis. In this paper, we report on the effects of exposure of compound biofilms of a primary colonizer *Streptococcus gordonii* combined with *F. nucleatum* on a hydroxyapatite substrate to iron oxide nanoparticles as possible bactericidal agent.

Keywords: Oral biofilms; Iron oxide nanoparticles; Bactericidal effects; *Fusobacterium nucleatum*; *Streptococcus gordonii*.

1. INTRODUCTION

Gingivitis and periodontitis are the most common types of adolescent and adult gum diseases and may result in tooth loss, gum recession, and bleeding upon probing, among many other adverse effects [Singh 2013], [Gupta 2013]. Gingivitis is an inflammation of the gums, without the loss of connective tissue. It is an extremely common oral disease, mostly caused by poor dental hygiene. Currently, the prescribed treatment for gingivitis is fairly inadequate and is entirely dependent on the patient to simply increase vigilance towards dental care at home. Gingivitis is seemingly harmless, preventable, and reversible, but if oral hygiene habits are poor, it may progress to a much more severe stage of periodontitis. Periodontitis manifests itself in permanent loss of bone and collagen structures supporting the teeth. It also increases risks of heart attack and stroke. Yet, its onset and progression can be stopped by proper oral hygiene and preventative treatment.

In 2012, data from the Center for Disease Control and Prevention estimated that 47.2% or 64.7 million of American adults suffered from periodontitis, the most dangerous and irreversible periodontal disease [Eke 2012]. Its prevalence increased to 70.1% of Americans aged 65 and older. Taking into account the progression of the disease, 8.7% (11.9 million) of American adults had mild periodontitis, 30% (41.1 million) had moderate periodontitis, and 8.5% (11.7 million) suffered from severe periodontitis. Most people with periodontitis are seldom aware that they have the disease. The wide spread of periodontitis is nationally overlooked due to its commonality. This causes massive concern for future dental care practices in periodontology.

Nanoparticles (NPs) have outstanding antimicrobial abilities, but are also infamously known to cause cytotoxicity and inflammation within the human body. For example, a recent study has shown that TiO_2 NPs can act as a successful antibacterial agent against gingival bacteria [Garcia-Contreras 2015]. However, as TiO_2 NPs infiltrated oral cells, they

Colloidal Nanoparticles for Biomedical Applications XIII, edited by Marek Osiński, Wolfgang J. Parak, Xing-Jie Liang, Proc. of SPIE Vol. 10507, 105070J · © 2018 SPIE
CCC code: 1605-7422/18/$18 · doi: 10.1117/12.2299280

enhanced gingival inflammation. This indicates dental treatment with TiO_2 NPs could have negative side effects, consistent with other reports of toxicity of TiO_2 NPs on blood cells [Khan 2015], [Kongseng 2016], renal system [Iavicoli 2016], lungs [Hanot-Roy 2016], [Schmid 2016], and central nervous system [Coccini 2015], [Hong 2015], [Czajka 2015], as well as their genotoxicity [Chen 2014], [Hanot-Roy 2016], [Kongseng 2016].

The poor quality of gingivitis treatment and the biomedical limitations of NPs such as TiO_2 indicate a need for the development of nontoxic substances that have increased potency as an antimicrobial agent but are safe enough to be used in household dental care products. In order to address this issue, we considered iron oxide NPs [Alas 2017]. Due to their biocompatibility, iron oxide NPs are being used in an increasing number of biomedical applications. For example, ferumoxytol (Feraheme™) NPs, consisting of a non-stoichiometric magnetite core surrounded by a polyglucose sorbitol carboxymethylether coating, have been approved by the U.S. Food and Drug Administration (FDA) for treatment of iron deficiency in patients with renal failure [Provenzano 2009], [Coyne 2009], [Lu 2010]. Various products containing iron-oxide NPs have also been approved by FDA for the use as contrast agents in magnetic resonance imaging [Wang 2015]. They are also found in a variety of biosensors and targeted drug delivery devices. Additionally, they have been demonstrated by several groups to have bactericidal activity against various species of bacteria [Tran 2010], [Behera 2012], [Prabhu 2015], [Armijo 2015], [Niemirowicz 2015]. According to a previous report, iron-oxide in NP form is not only non-toxic, but its byproduct, degraded iron from the cores, apparently accumulates in natural iron stores in the body [Weissleder 1989]. For these reasons, we have chosen to investigate whether Fe_3O_4 NPs can satisfy the need for a safe antimicrobial agent in oral hygiene and relieve the burden of lifetime disease management currently faced by patients with periodontitis.

We hypothesize that Fe_3O_4 NPs dispersed in commercial Listerine Coolmint mouthwash may prevent the onset of gingivitis while reducing the time required to be spent on daily oral hygiene, thus making dental care more efficient and appealing for many gingivitis patients. In our previous studies of using iron oxide NPs in treatment of cystic fibrosis, the NPs with an average diameter of 5-10 nm were shown to be able to penetrate thick bacterial biofilm and deliver antibiotics directly to the bacterial colonies [McGill 2009], [Brandt 2013], [Osiński 2013], [Armijo 2014]. We predict that a similar mechanism can be applied to oral bacterial biofilm, with Listerine Coolmint mouthwash as the main antiseptic. The NPs are anticipated to provide a mechanical component of the mouthwash that contributes to the penetration and disruption of colonizing secondary and tertiary colonizers, and thus prevents the formation of the detrimental tertiary layer.

1.1 Bactericidal effects of iron oxide NPs

Numerous studies have established that properly biofunctionalized Fe_3O_4 NPs can have bactericidal effect on *Staphylococcus aureus* [Tran 2010], [Behera 2012], [Prabhu 2015], [Darwish 2015], *Bacillus licheniformis*, *Staphylococcus epidermidis*, *Streptococcus aureus* [Behera 2012], *Bacillus subtilis* [Behera 2012], [Arakha 2015], *Escherichia coli* [Behera 2012], [Prabhu 2015], [Darwish 2015], [Arakha 2015], *Proteus vulgaris*, Xanthomonas [Prabhu 2015], and *Pseudonomas aeruginosa* [Armijo 2015], [Niemirowicz 2015]. The exact mechanism of the antimicrobial action of Fe_3O_4 NPs that results in damaging the bacterial proteins and DNA has not yet been determined, but it has been hypothesized that it might involve oxidative stress caused by reactive oxygen species, such as superoxide radicals (O_2^-), singlet oxygen ($^1O_2$), hydroxyl radicals (–OH), or hydrogen peroxide (H_2O_2) [Rudramurthy 2016]. For example, H_2O_2 could penetrate the cell membrane of the bacteria and kill the bacteria by entering the intracellular space.

It has also been established that bactericidal activity of Fe_3O_4 NPs strongly depends on the surface coating, and should be individually optimized for maximum effect on a particular bacterial species [Darwish 2015], [Arakha 2015]. For example, changing the zeta potential of as-synthesized iron oxide NPs from negative to positive by coating their surface with biocompatible chitosan has significantly increased their antimicrobial activity against Gram-positive *Bacillus subtilis* and Gram-negative *Escherichia coli*, reducing the percentage of viable cells after 22-hour exposure to 50 μM of NP suspension in nutrient broth from over 60% to less than 30% for either bacterial species [Arakha 2015]. Sensitivity to surface coating may also be a reason for large differences in results reported by various groups, as the NPs used in the experiments would often have different coatings.

1.2 Oral bacteria and onset of gingivitis

The human oral microbiome includes Gram-positive and Gram-negative bacteria, cocci, rods, filaments, spirochetes, *etc*. [Dewhirst 2010]. Most of the oral bacteria have never been cultured. Some of the oral microbes belong to very exotic taxonomic groups, for example archaea that are found in termite guts, hot springs, and other extreme environments. Along with the bacteria and archaea, oral microbiome also contains fungi and viruses. Most of the bacterial species are harmless, some are beneficial (such as probiotics assisting in food digestion), but some are responsible for various

diseases, primarily tooth decay and gum diseases such as gingivitis and periodontitis. For example, *Streptococus mutans* produces enamel-eroding acids, while *Porphyromonas gingivalis* is strongly linked to periodontitis.

Bacteria colonize a variety of surfaces in human mouth. Bacterial biofilms on tooth surfaces are known as dental plaque. It consists of at least 800 different bacterial species, and already in 2010 this number was expected to rise into the thousands with the advances in mass sequencing techniques [Filoche 2010]. Indeed, as of February 2016, the Human Oral Microbiome Database listed 1,200 predominant oral bacteria species, with some 19,000 phylotypes and with distinct subsets predominating in different habitats [Carrouel 2016].

Oral biofilms develop under a range of different conditions and various environments. In particular, dental plaque is a dynamic and extremely complex oral biofilm ecosystem. It is a structured multi-species community embedded in a matrix with water channels, with four distinct stages of development: attachment, growth, ecological succession, and maturation. Factors that affect dental plaque development include interbacterial co-adhesion, pH, level of oxygen, and availability of various nutrients. The microbial species in dental plaque form complex communities, with an assortment of micro-niches, metabolic functions, and inter- and intra-species interactions.

Development of dental plaque proceeds in three stages [Kolenbrander 2002]. Initially, Gram-positive early colonizers (*Streptococcus gordonii*, *Streptococcus mitis*, *Streptococcus oralis*, *Streptococcus sanguis*) bind via adhesins to complementary receptors in the acquired pellicle of saliva proteins coating the tooth surface. Then, Gram-negative secondary colonizers (*Fusobacterium nucleatum*) bind to previously bound primary colonizers, and provide a bridge through which a large group of late colonizers (*Actinobacillus actinomycetemcomitans*, *Actinomyces israelii*, *Actinomyces naeslundii*, *Capnocytophaga gingivalis*, *Capnocytophaga ochracea*, *Capnocytophaga sputigena*, *Eikenella corrodens*, *Eubacterium* spp, *Porphyromonas gingivalis*, *Prevotella denticola*, *Prevotella intermedia*, *Prevotella loescheii*, *Propionibacterium acnes*, *Selenomonas flueggei*, *Treponema denticola*, *Veillonella atypica*) can access the biofilm. Sequential binding of late colonizers results in the appearance of nascent surfaces that bridge with the next coaggregating partner cells.

Dental plaque comprises a complicated biofilm structure that varies from patient to patient, but a common factor in most cases is the single species of bacterium acting as a secondary colonizer, namely *Fusobacterium nucleatum*, while the actual disease is caused by a variety of tertiary colonizers. We hypothesize that the destruction of a compound biofilm containing *F. nucleatum* will prevent tertiary colonizers from establishing a harmful biofilm, and thus will protect the patient from developing gingivitis and, consequently, periodontitis.

2. SYNTHESIS AND CHARACTERIZATION OF Fe_3O_4 NANOPARTICLES

2.1 Synthesis of Fe_3O_4 nanoparticles

Numerous different approaches are available for the synthesis of Fe_3O_4 NPs, including co-precipitation, solvothermal or hydrothermal processing, sol-gel and forced hydrolysis, microemulsion processing, surfactant-mediated synthesis, laser pyrolysis, and electrochemical processing. We have chosen a solvothermal method that involves pyrolysis of iron (III) acetylacetonate ($Fe(acac)_3$) in high-boiling-point triethylene glycol (TREG) solvent, as it directly produces biocompatible water-soluble nanoparticles with a very high reaction yield. TREG plays a triple role of a solvent, reducing agent, and modifying agent in the reaction. The melting point of $Fe(acac)_3$ of 180-181 °C coincides with the onset of its thermal decomposition [Von Hoene 1958].

In our synthesis, $Fe(acac)_3$ dissolved in TREG was used as a precursor, resulting in highly crystalline magnetite (Fe_3O_4) NPs coated in TREG, with a typical size of 5-10 nm, depending on the reaction time and the ratio of $Fe(acac)_3$/TREG. The NPs were synthesized using the procedure of [Cai 2007], modified by increasing the molar fraction of $Fe(acac)_3$. The procedure consists of two steps: synthesis of the iron oxide NPs and the washing of the NPs in acetone. The washing procedure was taken from [Gonçalves 2010].

2.1.1 Materials. Iron (III) acetylacetonate ($Fe(acac)_3$, 97%), triethylene glycol (TREG, 99%), and acetone (99.5%) were purchased from Sigma-Aldrich, USA. All chemicals were used as received without purification.

2.1.2 Synthesis of iron oxide (magnetite) NPs. In a typical synthesis, 10.6 g (30 mmol) of $Fe(acac)_3$were added to 50 mL of TREG under continuous and vigorous stirring in a 250-mL three-neck flask attached to a condenser. The condenser was connected to a Schlenk line and placed under dry nitrogen flow. The mixture was then heated to the decomposition temperature of $Fe(acac)_3$ (180 °C) at a rate of 3 °C per minute under positive nitrogen pressure with continuous and vigorous stirring. The mixture was held at 180 °C for 30 minutes. The gaseous product of pyrolysis of $Fe(acac)_3$ is mostly acetone, with a slightly increasing fraction of CO_2 as the temperature is raised from 180 °C to 280 °C [Von Hoene 1958]. The temperature was then rapidly raised to the boiling point of TREG (270 °C) at rate of 10 °C per minute.

The mixture was held at 270 °C for two hours, during which time the NP growth occurred, with simultaneous reflux of TREG. The TREG solvent also acted as a surfactant, forming a protective hydrophilic layer on the NP surface. After the two hours, the flask was left to cool to room temperature. The NPs were washed in acetone several times and then dried to a powder. Fig. 1 illustrates the initial and final stages of the synthesis.

2.1.3 Washing of NPs. The excess of TREG after the reaction was removed through multiple steps of washing in acetone. The contents of the 3-neck flask were distributed into ten 20-mL scintillation vials and topped with acetone. Ultrasonic bath was used to disperse the NPs in the vials. A tandem of 8 rare-earth arc magnets was taped to the side of each vial, and the vials were left until the liquid became light brown. The magnets were then removed and the process was repeated 2-3 times until the liquid was clear. The vials were then left open overnight to let the remaining acetone evaporate. The remaining black powder was easily dispersible in deionized (DI) water. Fig. 2 illustrates the washing process.

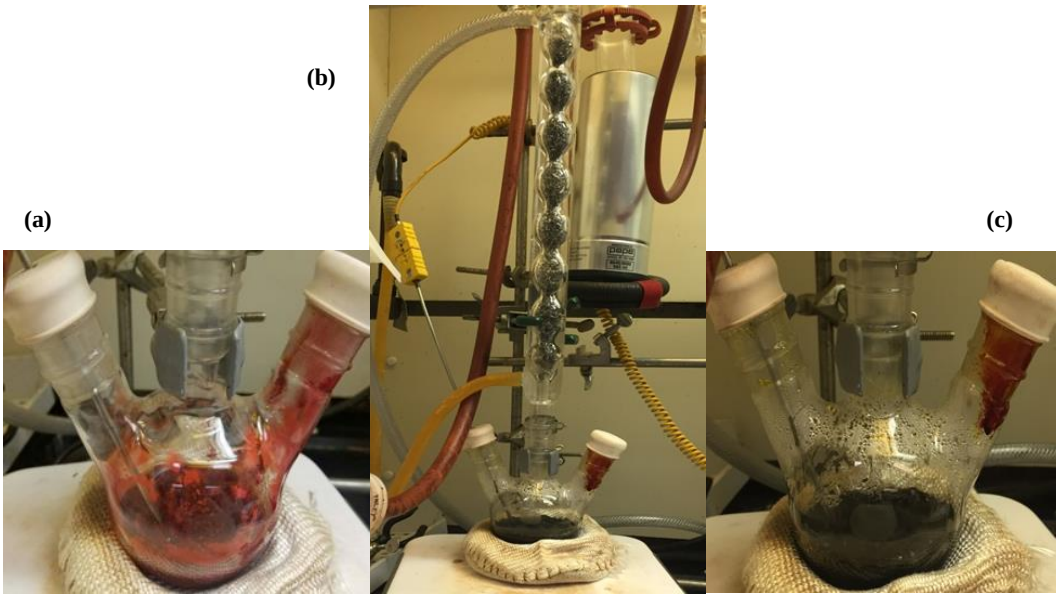

Fig. 1. (a) $Fe(acac)_3$ dissolved in TREG, prior to its pyrolysis. (b) Schlenk-line setup during the reaction, showing a condenser, a liquid nitrogen cold trap, and a thermocouple. (c) Final stage of the synthesis, with TREG refluxing during the process of NP growth.

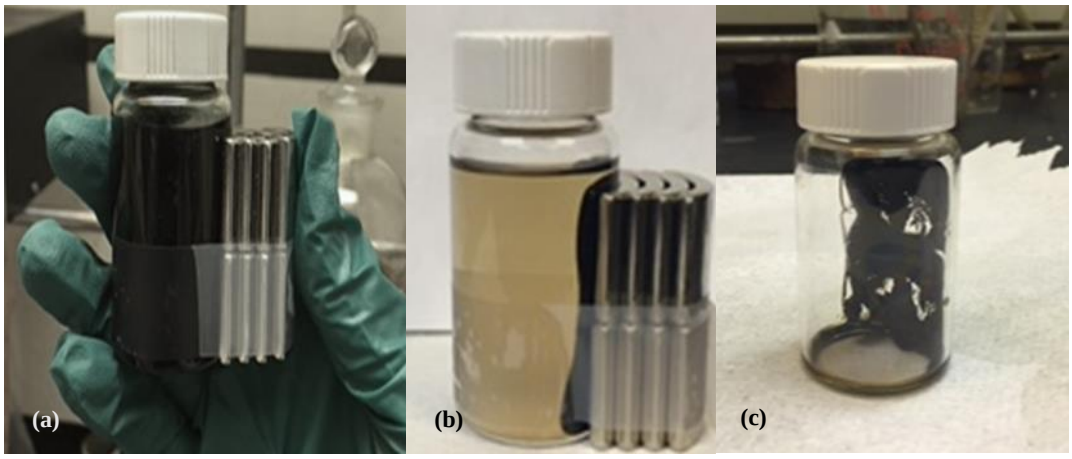

Fig. 2. (a) Appearance of scintillation vials after sonication. (b) Appearance of the vials shortly before decantation. (c) Appearance of the vials after decantation.

2.2 Characterization of Fe_3O_4 nanoparticles

2.2.1 Transmission electron microscopy. For structural characterization, samples for transmission electron microscopy (TEM) were prepared by placing a drop of the colloidal solution in water onto a 200-mesh carbon-backed copper grid

wetted with chlorobenzene. The liquid bilayer was allowed to evaporate away, thus fixing the NPs on the grid. High-resolution TEM (HRTEM) measurements were taken with a JEOL-2010F transmission electron microscope operating at 200 kV, with a charge-coupled device (CCD) camera attachment. The TEM was equipped with an OXFORD Link ISIS/Inca energy dispersive spectroscopy (EDS) apparatus, used to determine the elemental composition of the samples.

Fig. 3 shows an example of a TEM image of as-synthesized magnetite NPs. Their average size was ~5-10 nm. Most NPs were spherical, although some tended to be hexagonal in shape. The images display that the size distribution of the NPs was rather wide, which, we believe, should not affect their effectiveness in this particular application.

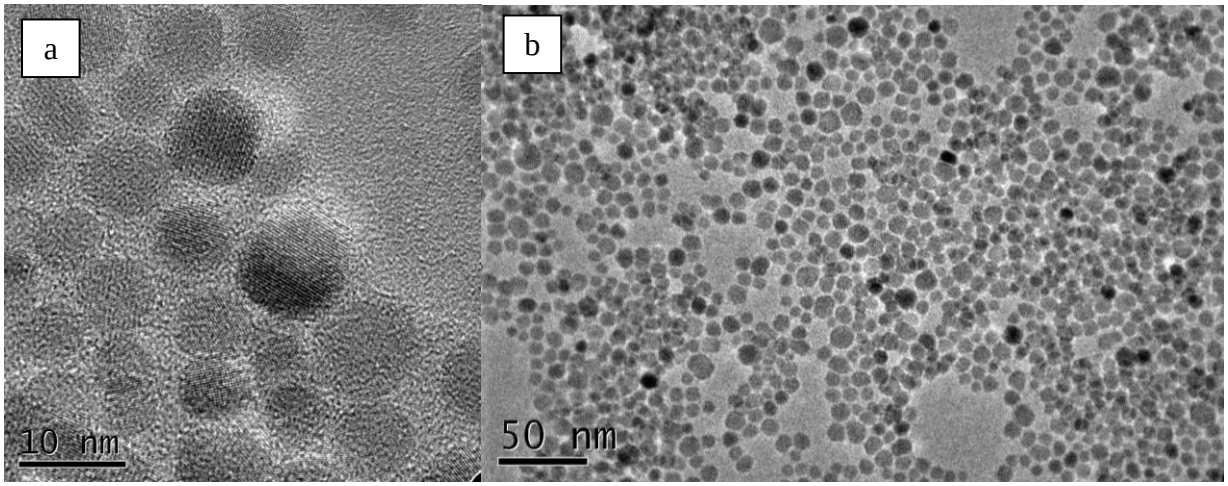

Fig. 3. TEM image of magnetite NPs. (a) Scale bar is 10 nm. (b) Scale bar is 50 nm.

2.2.2 Zeta potential analysis. Zeta potential was measured using a Malvern Zetasizer Nano-Z apparatus. The zeta potential is the electrokinetic potential that occurs at the interfacial double layer of a dispersing fluid surrounding a charged colloidal NP. It is measured from a slipping interface between a stationary layer of fluid attached to the NP and the bulk fluid away from that interface [Hunter 1988]. A colloidal suspension is considered to be electrostatically stable if the zeta potential is either greater than 20 mV or smaller than -20 mV. The zeta potential is measured by placing the sample in an electric field and measuring how fast, and in which direction, the NPs move between the anode and the cathode while suspended in a liquid solvent. Using this measurement, along with the known viscosity of the solvent, the Zetasizer is able to calculate the zeta potential, which is an indicator of the electrostatic stability of the NPs in a liquid.

The zeta potential of the NPs in DI water was measured to be 34.9 mV, indicating a stable colloidal suspension. However, when the NPs were placed in Listerine Coolmint mouthwash, the zeta potential decreased to -3.08 mV, which placed the NPs into the range of colloidal instability. This instability was also apparent in the flocculation and aggregation of the NPs once they were placed in the mouth rinse. Since the NPs were not stable in the mouth rinse and DI water is not advisable for human consumption, the colloidal stability of the NPs was alternatively tested in sterilized tap water. The zeta potential decreased further to -0.304 mV, which still indicated no colloidal stability. This was most likely due to the presence of minerals, ions, and other chemical components in the local tap water that influenced the pH levels of the NPs solution. To ensure that the NPs were colloidally stable in a solvent that is not biologically toxic, a mixture of DI water and sterilized tap water was created. The NPs were placed in a solution that comprised 87% of DI water and 13% of sterilized tap water and yielded a measurement of 21.7 mV, which placed the NPs on the border of the range of stability while reducing the acidity of DI water.

2.2.2 Thermogravimetric analysis. Thermogravimetric analysis and differential scanning calorimetry (TGA/DSC) are complementary techniques to investigate material's response to different temperatures: mass change (for example, at decomposition or sublimation temperatures) and thermal changes often unaccompanied by the mass change as a function of temperature (*e.g.*, melting, glass transition, heat capacity, enthalpy, and second-order phase transitions). We have used Netzsch STA 449 F1 Jupiter apparatus to determine mass fraction of the as-synthesized NPs that can be attributed to the Fe_3O_4 material, as opposed to the organic TREG coating.

The TGA results displayed in Fig. 4 indicate that ~10% of the mass of as-synthesized NPs was due to the organic coating. The onset of initial decomposition of TREG is 240 °C, consistent with an increased rate of loss of mass at 240.5 °C shown in Fig. 4.

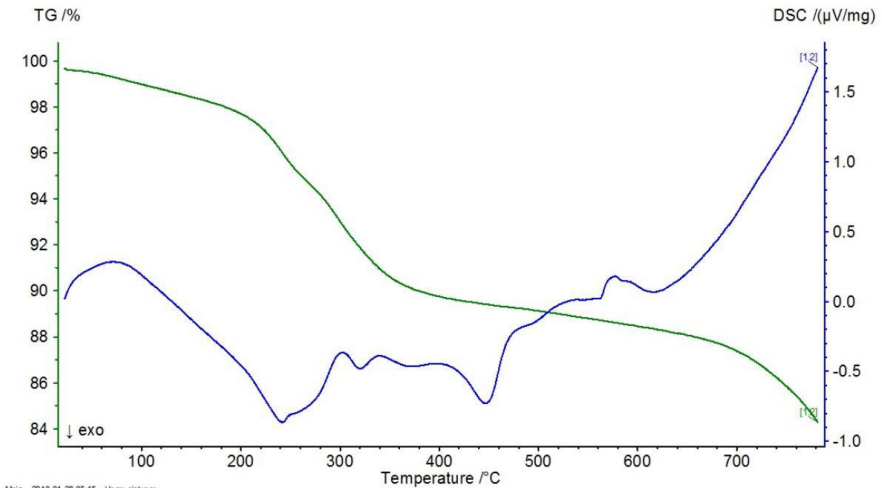

Fig. 4. Results of TGA and DSC analysis of Fe_3O_4/TREG NPs.

2.2.3 X-ray diffraction. Crystallographic structure of the Fe_3O_4 NPs was measured using a Rigaku Ultima III X-ray diffractometer. The results shown in Fig. 5 are consistent with the diffraction pattern of magnetite with the cubic Fd(-3)m space group, indicated by blue lines in Fig. 5.

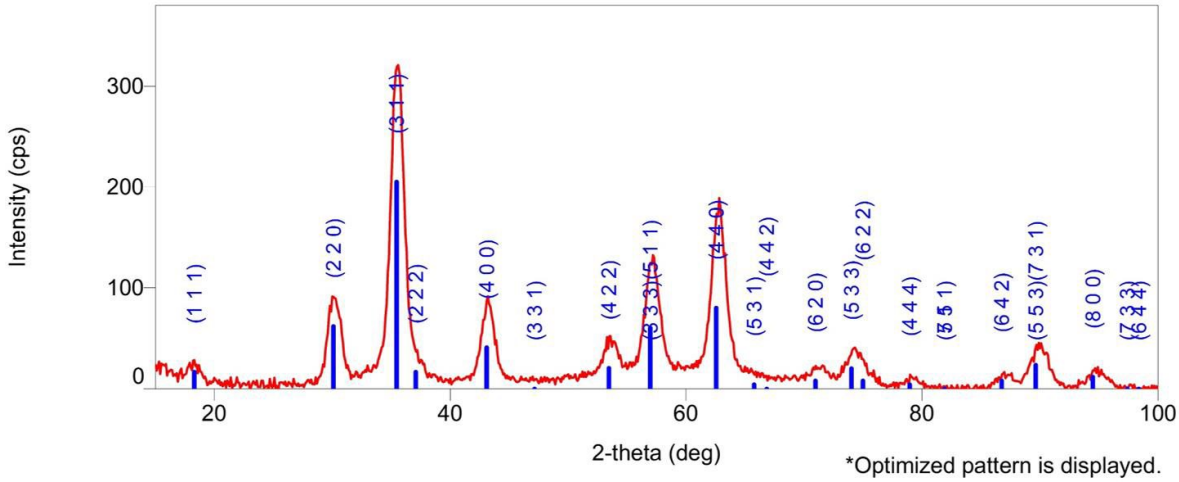

Fig. 5. Results of X-ray diffraction analysis of Fe_3O_4/TREG NPs. Blue lines represent the expected lines for the magnetite crystal.

2.3 Determination of reaction yield

The reaction yield was determined as follows. First, the amount of $Fe(acac)_3$ precursor added to the reaction flask was carefully weighed and converted into the initial number of moles of iron. Then, the weight of each empty scintillation vial was recorded, and compared with the weight of the same vials filled with the NP powder. The net difference was further reduced by 10%, based on the results of thermogravimetric analysis. The resultant weight of Fe_3O_4 NPs was then converted into the final number of moles of iron. The ratio of the final and initial numbers of moles of irons was taken as the reaction yield. In the particular case of the reaction described in Section 2.1, the reaction yield was 84%. In other batches, yields as high as 93% were obtained.

3. METHODOLOGY FOR BACTERIAL BIOFILM INVESTIGATIONS

3.1 Bacterial culturing methods

Strains of *S. gordonii* and *F. nucleatum* subspecies *polymorphum* were obtained through ATCC®. The strains were derived from the oral cavity of males with gingival inflammation. Each bacteria strain was used to inoculate commercial

anaerobic chopped meat media obtained from Fisher Scientific™. Each strain of bacteria was initially cultured separately, in order to develop planktonic bacteria shown in Figs. 6a and 6b. The media were then left to incubate at 37 °C under anaerobic conditions, obtained through the use of an anaerobic jar, until turbidity could be observed in the culturing vials (3-5 days). After the planktonic bacteria were cultured, they were then combined in a 1:1 ratio in fresh chopped meat media along with 7-mm-diameter hydroxyapatite discs. The discs served as the substrate for biofilm growth. Hydroxyapatite is the main mineral constituent found in human bone and teeth [Pepla 2014]. The cultures were maintained for another week until substantial biofilms could be observed at the bottom of the vials. Successful biofilm growth of *S. gordonii* and *F. nucleatum* is shown in Fig. 6(c).

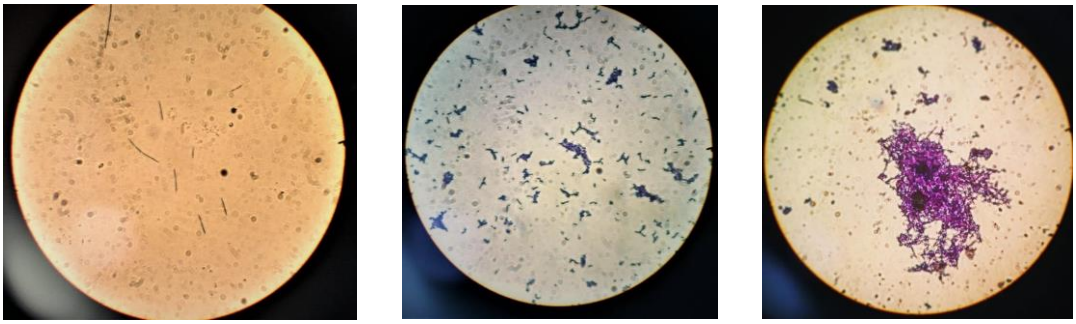

(a) (b) (c)

Fig. 6. Compound light microscope with oil immersion images of (a) *S. gordonii*; (b) *F. nucleatum*; and (c) compound biofilm of *S. gordonii* and *F. nucleatum* stained with crystal violet.

3.2 Determination of bactericidal ability of deionized water

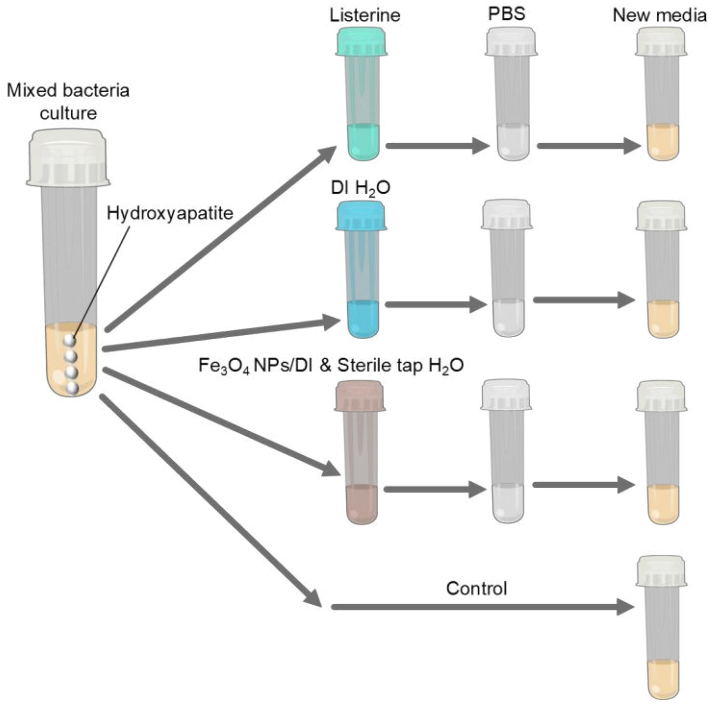

Fig. 7. Schematic of experimental procedure to test bactericidal abilities of DI water and NPs in mixture of DI water and sterile tap water compared to the Listerine Coolmint mouthwash.

The fact that our NPs were colloidally stable in DI water or in a mixture comprising DI water and up to 13% of sterilized tap water required additional control to determine possible contribution of DI water to anticipated bactericidal ability of the NP/water solution. Experimental procedures were developed to test the bactericidal effect of DI water on the compound biofilm of *F. nucleatum* and *S. gordonii* and compared the results to those of Listerine. The procedure, as outlined in Fig. 7, exposed one hydroxyapatite disc with the biofilm to pure DI water and one disc to Listerine Coolmint

mouthwash. The discs were exposed to the mouthwash for 30 and 90 seconds and to the DI water for 90 seconds. After exposure, the discs were immediately rinsed with phosphate-buffered saline (PBS) and subsequently placed in a vial of new media. The control in this experiment was hydroxyapatite discs placed in new media vials with no agitation. The vials were incubated anaerobically at 37 °C for 24 hours and absorbance measurements were performed.

3.3 Determination of exposure-time-dependent effects of Fe_3O_4 nanoparticles compared to Listerine

Since the NPs were not stable in the Listerine Coolmint mouthwash, experiments were conducted using the NPs in a mixture of 87% of DI water and 13% of sterilized tap water. As illustrated in Fig. 7, the bactericidal effects of this solution were compared to those of the Listerine Coolmint mouthwash and pure DI water, both not containing any NPs. Our previous studies have shown that the concentration of iron oxide NPs that resulted in the steepest decrease in bacterial metabolism was approximately 8 µg/mL [Alas 2017]. The experimental procedure in this paper utilized this concentration and kept it constant, while varying the exposure time of the bacteria to two solutions (Listerine alone, and iron oxide NPs in a mixture of DI and sterilized water). The range of times started at 30 seconds – which is the recommended time for rinsing per the instructions of Listerine – and increased in 30-second increments until a final time of 90 seconds.

Hydroxyapatite discs were extracted from the original culturing vial, containing compound biofilms of *F. nucleatum* and *S. gordonii*, and were placed into the two solutions. One disc was used for each type of solution and four trials were conducted with each solution at each exposure time. During the span of the exposure time, the vials were shaken by hand to simulate the swishing motion in the mouth when using mouth rinses. After exposure, the discs were immediately rinsed with PBS and were placed in vials containing new media. The control in this experiment comprised of no exposure time to any of the three solutions and contained one hydroxyapatite disc in new media. Four controls were made. In total, there were 24 trials conducted. All vials were then incubated anaerobically for 24 hours at 37 °C and were observed for turbidity. Turbidity was then quantified through absorption measurements.

4. RESULTS OF BACTERIAL BIOFILM INVESTIGATIONS

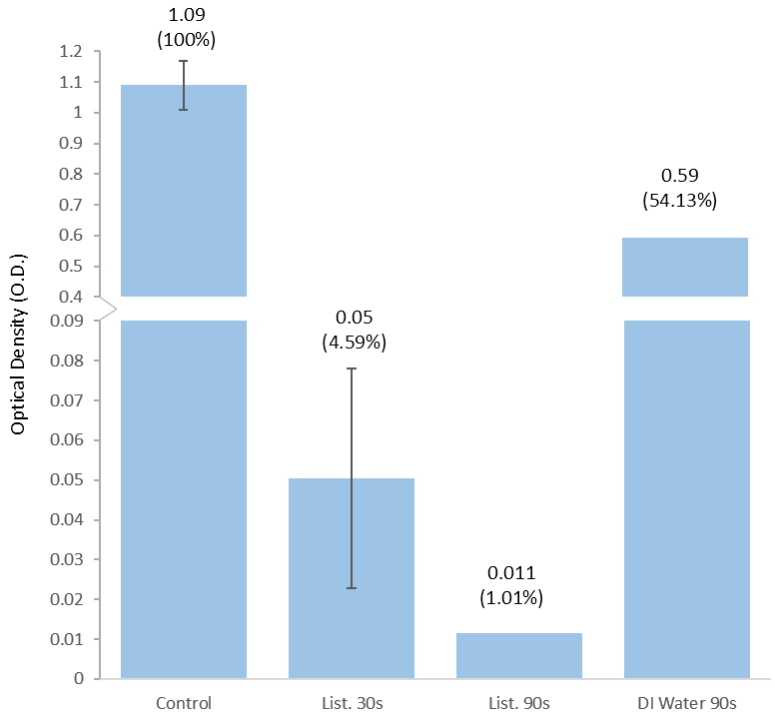

Fig. 8. Bar graph depicting comparisons between absorbance data for DI water at 90 seconds and Listerine Coolmint mouthwash at 30 and 90 seconds. Optical density of the control was used as basis of comparison.

4.1.1. Absorption measurements (Cary 5000 UV-Vis-NIR spectrophotometer). The optical density (OD) of each sample at 660 nm was measured and compared to that of the control, as shown in Fig. 8. The control had an OD of 1.09, which was treated as the basis for comparison. The bacteria experienced substantially lower recovery after exposure to the Listerine Coolmint mouthwash for 30 seconds, and this was further magnified in the results for 90 seconds in which the OD decreased to 1.01% of the control value of 1.09. In contrast, the exposure to DI water over 90 seconds only reduced the OD to 54.13%. While this indicates that DI water does display some bactericidal abilities, there is still plenty of room for additional contribution from the NPs to be quantified over the times scale of 90 s. The bactericidal effects of DI water alone are significantly weaker than those of the mouthwash alone or, as shown in Fig. 9, those of the solution containing the NPs diluted in the 87:13 mixture of DI water and sterilized tap water.

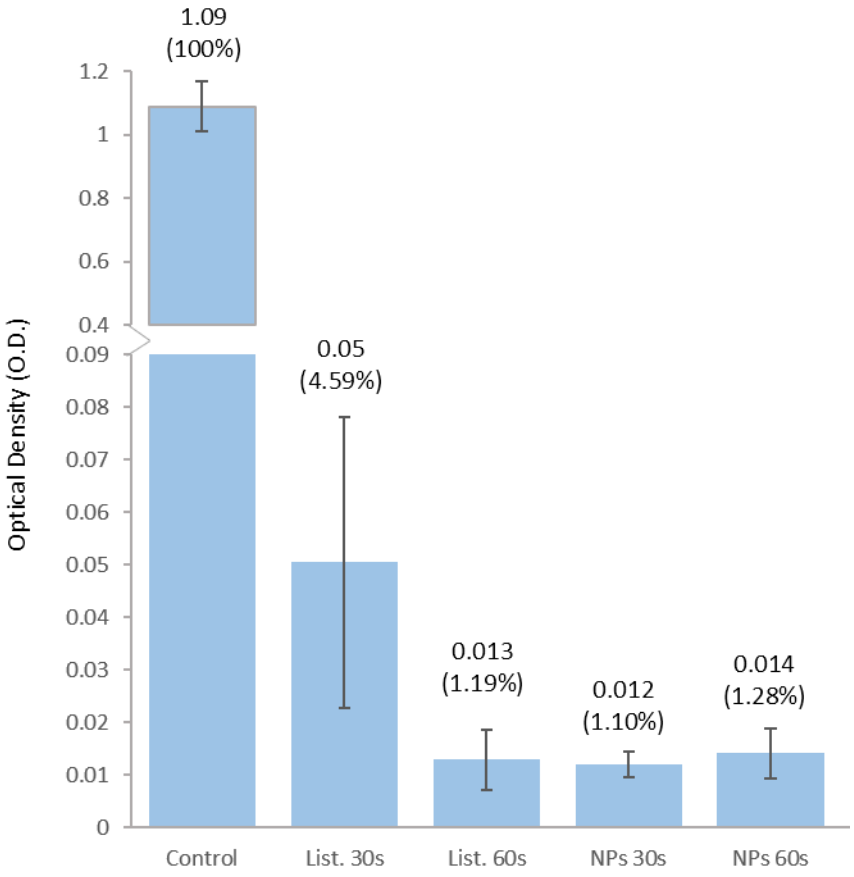

Fig. 9. Comparison of absorbance data between Listerine Coolmint mouthwash and iron oxide NPs in solution of DI water and sterilized water at 30 and 60 seconds. Optical density of control was used as basis for comparison.

The results in Fig. 9 display the absorbance data comparisons between the control, Listerine mouthwash, and the NPs solution at 30 and 60 seconds. Exposure to both the Listerine Coolmint mouthwash and the NPs decreased the OD at 660 nm significantly from the basis of 1.09. When comparing the mouthwash and NPs results at 30 seconds, the iron oxide NPs showed positive results in terms of yielding a lower OD at 1.1%, while the OD for the mouthwash was at 4.59% of the OD of the control. Yet, it can be observed from Fig. 9 that the differences in the OD after 60s are not significantly different from one another between the mouthwash and the NPs. A two-tailed Student's *t*-test was conducted on the absorbance data between the mouthwash and the NPs. With $N = 4$, the test yielded a *p*-value of 0.54 at 30 seconds and 0.85 at 60 seconds. This goes to conclude that the bactericidal effects of the NPs at the 8 μg/mL concentration are not significantly different from those of the Listerine Coolmint mouthwash.

5. ACKNOWLEDGEMENTS

Dr. Ying-Bing Jiang, Manager of the TEM/FIB Laboratory at the University of New Mexico (UNM), is acknowledged for his assistance with TEM measurements. The authors wish to express their gratitude to Dr. Ricardo H. Gonçalves from the Pennsylvania State University and to Dr. Karol Dokladny from the UNM Department of Internal Medicine, Division of Gastroenterology, for useful discussions.

This work was performed, in part, at the Center for Integrated Nanotechnologies, an Office of Science User Facility operated for the U.S. Department of Energy (DOE) Office of Science by Los Alamos National Laboratory and Sandia National Laboratories. Los Alamos National Laboratory, an affirmative action equal opportunity employer, is operated by Los Alamos National Security, LLC, for the National Nuclear Security Administration of the U.S. Department of Energy under contract DE-AC52-06NA25396. Sandia National Laboratories is a multi-mission laboratory managed and operated by National Technology and Engineering Solutions of Sandia, LLC., a wholly owned subsidiary of Honeywell International, Inc., for the U.S. Department of Energy's National Nuclear Security Administration under contract DE-NA-0003525.

6. REFERENCES

[Alas 2017] G. Alas, R. E. Pagano, J. Q. Nguyen, H. M. H. N. Bandara, S. A. Ivanov, G. A. Smolyakov, D. L. Huber, H. D. C. Smyth, and M. Osiński, "Effects of iron-oxide nanoparticles and magnetic fields on oral biofilms", *Colloidal Nanoparticles for Biomedical Applications XII* (M. Osiński, W. J. Parak, and X.-J. Liang, Eds.), SPIE International Symposium on Biomedical Optics BiOS 2017, San Francisco, CA, 28-30 Jan. 2017, *Proceedings of SPIE*, vol. 10078, Paper 1007806 (12 pp.).

[Arakha 2015] M. Arakha, S. Pal, D. Samantarrai, T. K. Panigrahi, B. C. Mallick, K. Pramanik, B. Mallick, and S. Jha, "Antimicrobial activity of iron oxide nanoparticle upon modulation of nanoparticle-bacteria interface", *Scientific Reports*, vol. 5, Art. 14813 (12+4 pp.), 6 Oct. 2015.

[Armijo 2014] L. M. Armijo, M. Kopciuch, Z. Olszówka, S. J. Wawrzyniec, A. C. Rivera, J. B. Plumley, N. C. Cook, Y. I. Brandt, D. L. Huber, G. A. Smolyakov, N. L. Adolphi, H. D. C. Smyth, and M. Osiński, "Delivery of antibiotics coupled to iron oxide nanoparticles across the biofilm of mucoid *Pseudonomas aeruginosa* and investigation of their efficacy", *Colloidal Nanoparticles for Biomedical Applications IX* (W. J. Parak, M. Osiński, and K. Yamamoto, Eds.), SPIE International Symposium on Biomedical Optics BiOS 2014, San Francisco, CA, 1-3 Feb, 2014, Proceedings of SPIE, vol. 8955, Paper 89550I (12 pp.).

[Armijo 2015] L. M. Armijo, P. Jain, A. Malagodi, F. Z. Fornelli, A. Hayat, A. C. Rivera, M. French, H. D. C. Smyth, and M. Osiński, "Inhibition of bacterial growth by iron oxide nanoparticles with and without attached drug: Have we conquered the antibiotic resistance problem?", *Colloidal Nanoparticles for Biomedical Applications X* (W. J. Parak, M. Osiński, and X.-J. Liang, Eds.), SPIE International Symposium on Biomedical Optics BiOS 2015, San Francisco, CA, 7-9 Feb. 2015, *Proceedings of SPIE*, vol. 9338, Paper 1Q (11 pp.).

[Bajpai 2014] I. Bajpai, K. Balani, and B. Basu, "Synergistic effect of static magnetic field and HA-Fe_3O_4 magnetic composites on viability of *S. aureus* and *E. coli* bacteria", *Journal of Biomedical Materials Research Part B: Applied Biomaterials*, vol. 102B, pp. 524-532, April 2014.

[Bandara 2010a] H. M. H. N. Bandara, J. Y. Y. Yau, R. M. Watt, L. J. Jin, and L. P. Samaranayake, "*Pseudonomas aeruginosa* inhibits *in-vitro Candida* biofilm development", *BMC Microbiology*, vol. 10, Art. 125 (9 pp.), April 2010.

[Bandara 2010b] H. M. H. N. Bandara, O. L. T. Lam, R. M. Watt, L. J. Jin, and L. P. Samaranayake, "Bacterial lipopolysaccharides variably modulate *in vitro* biofilm formation of *Candida* species", *Journal of Medical Microbiology*, vol. 59, pp. 1225-1234, 2010.

[Behera 2012] S. S. Behera, J. K. Patra, K. Pramanik, N. Panda, and H. Thatoi, "Characterization and evaluation of antibacterial activities of chemically synthesized iron oxide nanoparticles", *World Journal of Nano Science and Engineering*, vol. 2, pp. 196-200, Dec. 2012.

[Brandt 2013] Y. I. Brandt, L. M. Armijo, A. C. Rivera, J. B. Plumley, N. C. Cook, G. A. Smolyakov, H. D. C. Smyth, and M. Osiński, "Effectiveness of tobramycin conjugated to iron oxide nanoparticles in treating infection in cystic fibrosis", *Colloidal Nanoparticles for Biomedical Applications VIII* (W. J. Parak, M. Osiński, and K. Yamamoto, Eds.), SPIE International Symposium on Biomedical Optics BiOS 2013, San Francisco, CA, 2-4 Feb. 2013, *Proceedings of SPIE*, vol. 8595, Paper 85951C (9 pp.).

[Cai 2007] W. Cai and J. Q. Wan, "Facile synthesis of superparamagnetic magnetite nanoparticles in liquid polyols", *Journal of Colloid and Interface Science*, vol. 305, pp. 366-370, 2007.

[Carrouel 2016] F. Carrouel, S. Viennot, J. Santamaria, P. Veber, and D. Bourgeois, "Quantitative molecular detection of 19 major pathogens in the interdental biofilm of periodontally healthy young adults", *Frontiers in Microbiology*, vol. 7, Art. 840 (16 pp.), June 2016.

[Chen 2014] Z. J. Chen, Y. Wang, T. Ba, Y. Li, J. Pu, T. Chen , Y. S. Song, Y. E. Gu, Q. Qian, J. L. Yang, and G. Jia, "Genotoxic evaluation of titanium dioxide nanoparticles *in vivo* and *in vitro*", *Toxicology Letters*, vol. 226 (#3), pp. 314-3192 May 2014.

[Coccini 2015] T. Coccini, S. Grandi, D. Lonati, C. Locatelli, and U. De Simone, "Comparative cellular toxicity of titanium dioxide nanoparticles on human astrocyte and neuronal cells after acute and prolonged exposure", *NeuroToxicology*, vol. 48, pp. 77-89, May 2015.

[Coyne 2009] D. W. Coyne, "Ferumoxytol for treatment of iron deficiency anemia in patients with chronic kidney disease", *Expert Opinion on Pharmacotherapy*, vol. 10 (#15), pp. 2563-2568, 2009.

[Czajka 2015] M. Czajka, K. Sawicki, K. Sikorska, S. Popek, M. Kruszewski, and L. Kapka-Skrzypczak, "Toxicity of titanium dioxide nanoparticles in central nervous system", *Toxicology in Vitro*, vol. 29 (#5), pp. 1042-1052 Aug. 2015.

[Darwish 2015] M. S. A. Darwish, N. H. A. Nguyen, A. Ševců, and I. Stibor, "Functionalized magnetic nanoparticles and their effect on *Escherichia coli* and *Staphylococcus aureus*", *Journal of Nanomaterials*, vol. 2015, Art. 416012 (10 pp.), 2015.

[Dewhirst 2010] F. E. Dewhirst, T. Chen, J. Izard, B. J. Paster, A. C. R. Tanner, W.-H. Yu, A. Lakshmanan, and W. G. Wade, "The human oral microbiome", *Journal of Bacteriology*, vol. 192 (#19), pp. 5002-5017, Oct. 2010.

[Eke 2012] P. I. Eke, B. A. Dye, L. Wei, G. O. Thornton-Evans, and R. J. Genco, "Prevalence of periodontitis in adults in the United States: 2009 and 2010", *Journal of Dental Research*, vol. 91 (#10), pp. 914-920, 2012.

[Filoche 2010] S. Filoche, L. Wong, and C. H. Sissons, "Oral biofilms: Emerging concepts in microbial ecology", *Journal of Dental Research*, vol. 89 (#1), pp. 8-18, 2010.

[Garcia-Contreras 2015] R. Garcia-Contreras, M. Sugimoto, N. Umemura, M. Kaneko, Y. Hatakeyama, T. Soga, M. Tomita, R. J. Scougall-Vilchis, R. Contreras-Bulnes, H. Nakajima, and H. Sakagami, "Alteration of metabolomic profiles by titanium dioxide nanoparticles in human gingivitis model", *Biomaterials*, vol. 57, pp. 33-40, July 2015.

[Gonçalves 2010] R. H. Gonçalves, C. A. Cardoso, and E. R. Leite, "Synthesis of colloidal magnetite nanocrystals using high molecular weight solvent", *Journal of Materials Chemistry*, vol. 20 (#6), pp. 1167-1172 (2010).

[Gupta 2013] K. D. Gupta, N. Ahmad, and P. Gupta, *Gingival and Periodontal Diseases in Children and Adolescents*, LAP Lambert Academic Publishing, Oct. 2013.

[Hanot-Roy 2016] M. Hanot-Roy, E. Tubeuf, A. Guilbert, A. Bado-Nilles, P. Vigneron, B. Trouiller, A. Braun, and G. Lacroix, "Oxidative stress pathways involved in cytotoxicity and genotoxicity of titanium dioxide (TiO_2) nanoparticles on cells constitutive of alveolo-capillary barrier *in vitro*", *Toxicology in Vitro*, vol. 33, pp. 125-135, June 2016.

[Hong 2015] F. S. Hong, L. Sheng, Y. G. Ze, J. Hong, Y. J. Zhou, L. Wang, D. Liu, X. H. Yu, B. Q. Xu, X. Y. Zhao, and X. Ze, "Suppression of neurite outgrowth of primary cultured hippocampal neurons is involved in impairment of glutamate metabolism and NMDA receptor function caused by nanoparticulate TiO_2", *Biomaterials*, vol. 53, pp. 76-85, June 2015.

[Hunter 1988] R. J. Hunter, *Zeta Potential in Colloid Science: Principles and Applications*, Academic Press, 1988.

[Iavicoli 2016] I. Iavicoli, L. Fontana, and G. Nordberg, "The effects of nanoparticles on the renal system", *Critical Reviews in Toxicology*, vol. 46 (#6), pp. 490-560, 2016.

[Khan 2015] M. Khan, A. H. Naqvi, and M. Ahmad, "Comparative study of the cytotoxic and genotoxic potentials of zinc oxide and titanium dioxide nanoparticles", *Toxicology Reports*, vol. 2, pp. 765-774, 2015.

[Kolenbrander 2002] P. E. Kolenbrander, R. N. Andersen, D. S. Blehert, P. G. Egland, J. S. Foster, and R. J. Palmer Jr., "Communication among oral bacteria", *Microbiology and Molecular Biology Reviews*, vol. 66 (#3), pp. 486-505, Sept. 2002.

[Kongseng 2016] S. Kongseng, K. Yoovathaworn, K. Wongprasert, R. Chunhabundit, P. Sukwong, and D. Pissuwan, "Cytotoxic and inflammatory responses of TiO_2 nanoparticles on human peripheral blood mononuclear cells", *Journal of Applied Toxicology*, vol. 36 (#10), pp. 1364-1373, Oct. 2016.

[Lu 2010] M. Lu, M. H. Cohen, D. Rieves, and R. Pazdur, "FDA report: Ferumoxytol for intravenous iron therapy in adult patients with chronic kidney disease", *American Journal of Hematology*, vol. 85 (#5), pp. 315-319, May 2010.

[Martin 2012] G. C. Martin, *Development of an Orally Relevant Biofilm Disinfection Model*, Ph.D. Dissertation, University College London, UK, 2012 (660 pp.).

[McGill 2009] S. L. McGill, C. Cuylear, N. L. Adolphi, M. Osiński, and H. Smyth, "Enhanced drug transport through alginate biofilms using magnetic nanoparticles", *Colloidal Quantum Dots for Biomedical Applications IV* (M. Osiński, T. M. Jovin, and K. Yamamoto, Eds.), SPIE International Symposium on Biomedical Optics BiOS 2009, San Jose, CA, 24-26 Jan. 2009, *Proceedings of SPIE*, vol. 7189, Paper 718918 (8 pp.).

[Niemirowicz 2015] K. Niemirowicz, U. Surel, A. Z. Wilczewska, J. Mystkowska, E. Piktel, X. B. Gu, Z. Namiot, A. Kułakowska, P. B. Savage, and R. Bucki, "Bactericidal activity and biocompatibility of ceragenin-coated magnetic nanoparticles", *Journal of Nanobiotechnology*, vol. 13, Art. 32 (11 pp.), 1 May 2015.

[Osiński 2013] M. Osiński, Y. I. Brandt, L. M. Armijo, M. Kopciuch, N. J. Withers, N. C. Cook, N. L. Adolphi, G. A. Smolyakov, and H. D. C. Smyth, "Efficacy of tobramycin conjugated to superparamagnetic iron oxide nanoparticles in treating cystic fibrosis infections (Invited Paper)", *Low-Dimensional Semiconductor Structures* (T. V. Torchynska, L. Khomenkova, G. Polupan, and G. Burlak, Eds.), XXII International Material Research Congress 2013 (IMRC 2013), Cancún, Mexico, 11-15 Aug. 2013, *MRS Proceedings*, vol. 1617 (11 pp.)

[Pepla 2014] E. Pepla, L. K. Besharat, G. Tenore, and G. Migliau. "Nano-hydroxyapatite and its applications in preventive, restorative and regenerative dentistry: a review of literature", *Annali di Stomatologia*, vol. 5 (#3), pp. 108-114, Nov. 2014.

[Prabhu 2015] Y. T. Prabhu, K. V. Rao, B. S. Kumari, V. S. S. Kumar, and T. Pavani, "Synthesis of Fe_3O_4 nanoparticles and its antibacterial application", *International Nano Letters*, vol. 5, pp. 85-92, 2015.

[Provenzano 2009] R. Provenzano, B. Schiller, M. Rao, D. Coyne, L. Brenner, and B. J. Pereira, "Ferumoxytol as an intravenous iron replacement therapy in hemodialysis patients" *Clinical Journal of the American Society of Nephrology*, vol. 4 (#2), pp. 386-93, Feb. 2009.

[Rudramurthy 2016] G. R. Rudramurthy, M. K. Swamy, U. R. Sinniah, and A. Ghasemzadeh, "Nanoparticles: Alternatives against drug-resistant pathogenic microbes", *Molecules*, vol. 21 (#7), Art. 836 (30 pp.), 2016.

[Schmid 2016] O. Schmid and T. Stoeger, "Surface area is the biologically most effective dose metric for acute nanoparticle toxicity in the lung", *Journal of Aerosol Science*, vol. 99, Special Issue, pp. 133-143, Sept. 2016.

[Singh 2013] D. K. Singh, *Epidemiology of Gingival and Periodontal Diseases*, LAP Lambert Academic Publishing, Jan. 2013.

[Tran 2010] N. Tran, A. Mir, D. Mallik, A. Sinha, S. Nayar, and T. J. Webster, "Bactericidal effect of iron oxide nanoparticles on *Staphylococcus aureus*", *International Journal of Nanomedicine*, vol. 5, pp. 277-283, 2010.

[Von Hoene 1958] J. Von Hoene, R. G. Charles, and W. M. Hickam, "Thermal decomposition of metal acetylacetonates. Mass spectrometer studies", *Journal of Physical Chemistry*, vol. 62 (#9), pp. 1098-1101, Sept. 1958.

[Wang 2015] Y.-X. J. Wang, "Current status of superparamagnetic iron oxide contrast agents for liver magnetic resonance imaging", *World Journal of Gastroenterology*, vol. 21 (#47), pp. 13400-13402, 21 Dec. 2015

[Weissleder 1989] R. Weissleder, D. D. Stark, B. L. Engelstad, B. R. Bacon, C. C. Compton, D. L. White, P. Jacobs, and J. Lewis, "Superparamagnetic iron oxide: Pharmacokinetics and toxicity", *American Journal of Roentgenology*, vol. 152 (#1), pp. 167-173, 1 Jan. 1989.